PHYSICAL REVIEW C **88**, 051304(R) (2013)

Electromagnetic properties of the 2_1^+ state in ^{134}Te: Influence of core excitation on single-particle orbits beyond ^{132}Sn

A. E. Stuchbery,[1] J. M. Allmond,[2] A. Galindo-Uribarri,[3,4] E. Padilla-Rodal,[5] D. C. Radford,[3] N. J. Stone,[4,6] J. C. Batchelder,[7] J. R. Beene,[3] N. Benczer-Koller,[8] C. R. Bingham,[3,4] M. E. Howard,[8] G. J. Kumbartzki,[8] J. F. Liang,[3] B. Manning,[8] D. W. Stracener,[3] and C.-H. Yu[3]

[1]*Department of Nuclear Physics, RSPE, The Australian National University, Canberra ACT 0200, Australia*
[2]*Joint Institute for Heavy Ion Research, Oak Ridge National Laboratory, Oak Ridge, Tennessee 37831, USA*
[3]*Physics Division, Oak Ridge National Laboratory, Oak Ridge, Tennessee 37831, USA*
[4]*Department of Physics and Astronomy, University of Tennessee, Knoxville, Tennessee 37996, USA*
[5]*Instituto de Ciencias Nucleares, UNAM, AP 70-543, 04510 México, D.F., México*
[6]*Department of Physics, Oxford University, Oxford, OX1 3PU, United Kingdom*
[7]*UNIRIB, Oak Ridge Associated Universities, Oak Ridge, Tennessee 37831, USA*
[8]*Department of Physics and Astronomy, Rutgers University, New Brunswick, New Jersey 08903, USA*

(Received 23 June 2013; revised manuscript received 22 October 2013; published 15 November 2013)

The g factor and $B(E2)$ of the first excited 2^+ state have been measured following Coulomb excitation of the neutron-rich semimagic nuclide ^{134}Te (two protons outside ^{132}Sn) produced as a radioactive beam. The precision achieved matches related g-factor measurements on stable beams and distinguishes between alternative models. The $B(E2)$ measurement exposes quadrupole strength in the 2_1^+ state beyond that predicted by current large-basis shell-model calculations. This additional quadrupole strength can be attributed to coupling between the two valence protons and excitations of the ^{132}Sn core. However, the wave functions of the low-excitation positive-parity states in ^{134}Te up to 6_1^+ remain dominated by the $\pi(g_{7/2})^2$ configuration.

DOI: 10.1103/PhysRevC.88.051304 PACS number(s): 25.70.De, 23.20.−g, 21.10.Ky, 27.60.+j

Nuclei with a few protons or neutrons outside a double-magic closed-shell nucleus are of special interest because the spectroscopy of their few-particle excitations gives important insights into the properties of the nucleon orbits, as well as the extent to which the core is inert. This Rapid Communication reports on the Coulomb excitation of a radioactive beam of ^{134}Te ($T_{1/2} = 42$ min), the semimagic $N = 82$ nucleus with two protons outside the neutron-rich, double-magic nucleus ^{132}Sn. Despite the expected simple two-proton character of ^{134}Te, the theoretical predictions of the g factor of the first excited state range from 0.5 to 0.86 [1–4]. Both the gyromagnetic ratio (or g factor) of the 2_1^+ state and the reduced transition probability, $B(E2; 0_1^+ \rightarrow 2_1^+) = B(E2)\uparrow$, were measured.

Gyromagnetic ratio measurements on excited states of radioactive beams are challenging, and very few cases have been measured. The recoil in vacuum (RIV) method was first applied to a radioactive beam of ^{132}Te by Stone *et al.* [5]. We recently reported $B(E2)\uparrow$ and $g(2_1^+)$ measurements on the neutron-rich isotopes ^{126}Sn and ^{128}Sn [6–8]. The $B(E2)\uparrow$ measurement for ^{134}Te was a pioneering case of Coulomb excitation on radioactive beams [9,10]. Here the precision has been improved significantly. The present work on ^{134}Te represents an advance in RIV g-factor measurements: ^{134}Te is further from stability, only two nucleons away from ^{132}Sn, and being semimagic has a relatively low excitation probability. Even so, the measured g factor has a precision that rivals traditional measurements on stable beams. Moreover, it distinguishes between the alternative models [1–4], and the precise $B(E2)$ measured simultaneously reveals an unexpected level of quadrupole collectivity in the first excited state.

The measurements were performed at the Holifield Radioactive Ion Beam Facility (HRIBF). Beams of ^{130}Te and radioactive ^{134}Te (94.4% pure), at an energy of 390 MeV, were Coulomb excited on a $\sim$1 mg/cm^2 natural C target. The ^{130}Te beam was also excited at 342.8 MeV on the C target to check that the Coulomb excitation was "safe." A Bragg detector placed behind the target measured the energy loss of the 390-MeV ^{130}Te beam in the target to be 86(1) MeV. The ^{134}Te beam, with intensity near 10^7 ions/s, was incident on the target for $\sim$3 days. Some data were taken for the ^{134}Te beam excited on an $\sim$0.8 mg/cm^2 Mylar target.

Recoiling target nuclei were detected in three rings of the "bare" HyBall array (BareBall) [11], namely, ring $2 = 14^\circ - 28^\circ$ relative to the beam direction, ring $3 = 28^\circ - 44^\circ$, and ring $4 = 44^\circ - 60^\circ$. BareBall is a minimum-absorber, 2π version of HyBall. Coincident γ rays were detected in three rings of the CLARION array [12], which was configured with five Compton suppressed Clover detectors at 90°, three at 132°, and two or one at 154° for the ^{134}Te and ^{130}Te beams, respectively. The Clover detectors were at a distance of 21.75 cm from the target. The experimental trigger required either scaled-down particle singles or a particle-γ coincidence.

The total particle-gated γ-ray spectra for excitation of the 390-MeV beams are shown in Fig. 1. Whereas the $B(E2)$ is determined primarily by the ratio of the total γ-ray intensity to Rutherford scattering, the g-factor measurement requires a detailed analysis of the particle-γ angular correlations. In the presence of vacuum deorientation, the particle-γ angular correlation takes the form (see, e.g., Ref. [13] and references therein) $W(\theta_p, \theta_\gamma, \Delta\phi) = 1 + \sum_{kq} B_{kq}(\theta_p) Q_k G_k F_k D_{q0}^{k*}(\Delta\phi, \theta_\gamma, 0)$, where θ_p and θ_γ are the polar detection angles for particles and γ rays, respectively. $\Delta\phi = \phi_\gamma - \phi_p$ is the difference between the corresponding azimuthal detection angles. The attenuation coefficients G_k

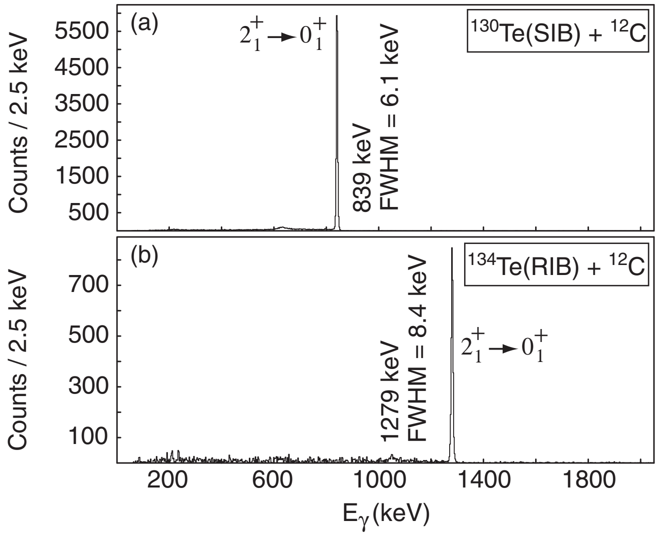

FIG. 1. Carbon-gated and Doppler-corrected γ-ray spectra for (a) stable ^{130}Te and (b) radioactive ^{134}Te.

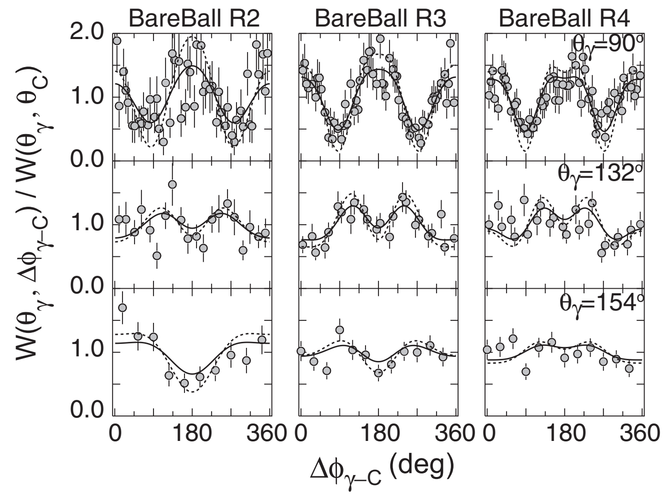

FIG. 2. Angular correlations for ^{134}Te excited on C. The unperturbed correlation is shown by the dashed curve; solid lines show the best fit to the attenuated correlations.

specify the vacuum deorientation effect, and $B_{kq}(\theta_p)$ is the statistical tensor, which defines the spin alignment of the initial state. F_k represents the usual F coefficient for the γ-ray transition, and Q_k is the attenuation factor for the finite size of the γ-ray detector. $D^{k*}_{q0}(\Delta\phi, \theta_\gamma, 0)$ is the rotation (Wigner-D) matrix. For $E2$ excitation, the "rank" k is $k = 2, 4$ and $-k \leqslant q \leqslant k$.

The three rings of the BareBall array and the three rings of the CLARION array were used to construct nine particle-γ angular correlations in $\Delta\phi$. Results for the ^{134}Te beam excited on the C target are shown in Fig. 2. The angular correlations for ^{130}Te are very similar to those published previously [5]. Examples of unperturbed angular correlations have also been given in Ref. [5]. Analysis procedures followed those described for the $B(E2)$ and g-factor measurements on $^{124-128}$Sn [6,7]. The stopping powers for Te in carbon used in the analysis were chosen to reproduce both the measured energy loss in the target and the observed γ-ray Doppler shifts. Results are summarized in Table I, which includes comparisons with previous $B(E2)$ values [9,10,14,15]. It can be seen that the present results are in excellent agreement with the previous measurements, and that the precision of the $B(E2)$ for ^{134}Te has been improved by a factor of three.

The product of the g factor and level lifetime, $|g|\tau$, was determined directly from fits to the angular correlations by expressing the attenuation coefficients G_2 and G_4 as a function of $|g|\tau$. To calibrate the hyperfine interactions, the present results for 390-MeV ^{130}Te excited on C, under the same experimental conditions as the ^{134}Te measurement, were combined with previous RIV calibration data for Te ions obtained using the BareBall and CLARION arrays [5,7]. The fitting procedure is illustrated in Fig. 3. A model-based fit to the calibration data on ^{122}Te, ^{126}Te, and ^{130}Te has been used to extrapolate towards $|g|\tau = 0$, as described in Ref. [7]. The resultant g factor for ^{134}Te is not very sensitive to the exact functional form assumed for the G_k versus $|g|\tau$ curve. For example, in a previous analysis of the g factor of ^{132}Te, it was assumed that $G_k = C_k/(C_k + |g|\tau)$, where the C_k parameters were fitted to the calibration data on the stable Te isotopes [16]. An analysis of the ^{134}Te data using this purely empirical approach gives results that differ by a negligible amount (about 1%) from the present, more refined, procedures.

TABLE I. Summary of results.

Nuclide	E_{beam} (MeV)	Target	$B(E2)\uparrow$ (e^2 b^2) Present	$B(E2)\uparrow$ (e^2 b^2) Previous[a]	$\|g\|\tau$ (ps)	$\tau(2_1^+)$ (ps)	$g(2_1^+)$
^{130}Te	343	C	0.280(12)			3.50(15)	
	390	C	0.292(10)			3.36(11)	
			0.291(10)[b]	0.295(7)		3.37(11)[b]	
^{134}Te	390	C	0.104(4)	0.116(12)	0.83(9)	1.14(5)	
		Mylar			1.0(2)		
					0.87(8)[b]		(+)0.76(9)[c]

[a]Value for ^{130}Te from [14]; value for ^{134}Te is an average of 0.114(13) [9,15], and 0.13(4) [10].
[b]Average value.
[c]Includes ±6% uncertainty in hyperfine field strength.

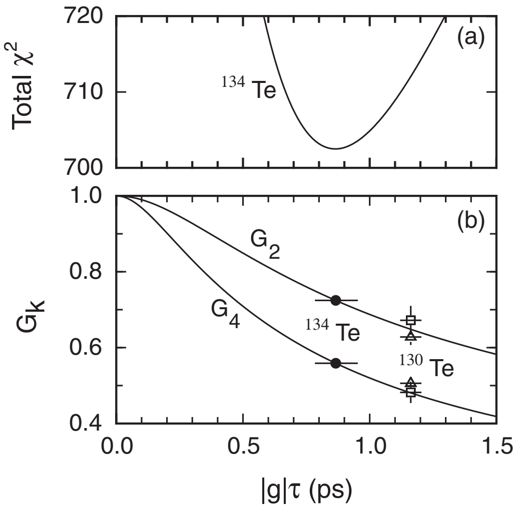

FIG. 3. (a) Total χ^2 (for both targets) versus $|g|\tau$ for ^{134}Te. $\chi_\nu^2(\text{min}) = 1.03$. (b) G_k versus $|g|\tau$ calibration curves for BareBall ring 3. The best fit $|g|\tau$ value for ^{134}Te, and its uncertainty, is projected onto the curves (filled circles). Also shown are the present BareBall ring-3 data (squares) and the data from [5] (triangles) for ^{130}Te which, together with additional measurements [7], define the calibration curves [16].

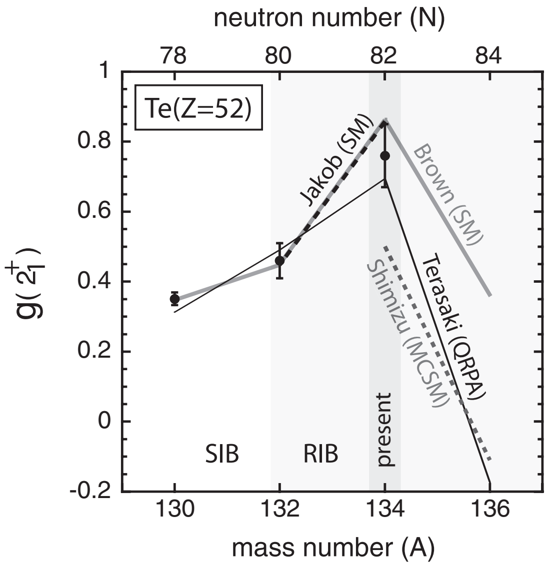

FIG. 4. Theoretical g factors in the even Te isotopes near $N = 82$ compared with experiment [5,15–17]. Jakob *et al.* [1] and Brown *et al.* [3] performed shell-model (SM) calculations. Terasaki *et al.* [2] used the quasiparticle random phase approximation (QRPA), and Shimizu *et al.* [4] used a Monte Carlo shell-model (MCSM) approach.

An additional cross-check on the reliability of the calibration procedures is provided by the comparison, in Ref. [7], of our recent RIV g-factor measurement on ^{124}Sn with independent transient-field measurements. In the case of ^{124}Sn, the required extrapolation is much larger than required here.

An uncertainty of $\pm 6\%$, which originates mainly from the uncertainties in the adopted g factors of ^{130}Te and ^{126}Te [17], is assigned to the calibration of the hyperfine field strength [7]. The present $g(2_1^+)$ measurement on the radioactive beam matches the typical precision of the $g(2_1^+)$ measurements on the stable $N = 82$ isotones between $^{136}_{56}$Xe and $^{144}_{62}$Sm [18]. Although the RIV method does not determine the sign of the g factor, a positive value for $g(2_1^+)$ in ^{134}Te is beyond dispute.

Figure 4 shows the experimental [5,15–17] and theoretical [1–4] $g(2_1^+)$ systematics for the Te isotopes near $N = 82$. There is good agreement between theory and experiment for ^{130}Te and ^{132}Te; however, the theories do not agree for ^{134}Te. Nevertheless, the two shell-model calculations [1,3] and the quasiparticle random phase approximation (QRPA) calculation [2] in fact predict similar wave functions, dominated by the $\pi(g_{7/2})^2$ configuration. The difference in predicted g factors comes from the use of different $M1$ operators. The $M1$ operator can be written as

$$\boldsymbol{\mu} = (g_l + \delta g_l)\boldsymbol{\ell} + (g_s + \delta g_s)\boldsymbol{s} + g_p[\boldsymbol{Y}_2, \boldsymbol{s}]_1, \qquad (1)$$

where g_l and g_s are the bare-nucleon orbital and spin g factors, respectively. The anomalous orbital magnetism of the nucleon δg_l arises principally from meson-exchange effects, whereas the anomalous spin g factor δg_s and the tensor component g_p are mainly from first-order core-polarization effects. In principle, δg_l, δg_s, and g_p all vary from orbit to orbit and from nucleus to nucleus. In practice, it is common to adopt "universal" values of δg_l and δg_s across a range of nuclei. It is also common to ignore the tensor term, i.e., put $g_p = 0$, as well as to set $\delta g_l = 0$, and choose δg_s so that the effective spin g factor is quenched to about 0.7 times that of the free nucleon [2,4].

The earlier shell-model calculations on the Te isotopes [1] ignored the tensor term and chose the orbital and spin g factors, $\delta g_l = 0.13$ and $\delta g_s = -1.55$ (or $g_s + \delta g_s = 4.04 = 0.72 g_s^{\text{free}}$), to reproduce the g factors of the low-lying $7/2^+$ ($\pi g_{7/2}$) and $5/2^+$ ($\pi d_{5/2}$) states in the odd-Z, $N = 82$ isotones near ^{132}Sn. The more recent work of Brown *et al.* [3] explicitly calculated the orbit-dependent core-polarization and meson-exchange corrections to the $M1$ operator for nuclei adjacent to ^{132}Sn. For the $\pi g_{7/2}$ and $\pi d_{5/2}$ orbits, Brown *et al.* [3] have quite different values of $\delta g_l(\pi g_{7/2}) = 0.113$ and $\delta g_l(\pi d_{5/2}) = 0.047$, whereas the values of $\delta g_s \sim -2.1$ and $g_p \sim 1.6$ are similar for both orbits.

Despite the simplification of orbit-independent corrections in Ref. [1], the calculated g factors for the lowest 2^+, 4^+, and 6^+ states in ^{132}Te and ^{134}Te are in close agreement with those of Brown *et al.* [3]. This agreement comes about because the g factor of the $\pi g_{7/2}$ orbit ($\ell = 4$) is strongly affected by δg_l, whereas the g factor of the $\pi d_{5/2}$ orbit ($\ell = 2$) is less sensitive.

In contrast with these shell-model calculations, the QRPA calculations of Terasaki *et al.* [2] use $g_p = 0$, $\delta g_l = 0$, and quench the spin g factor to 0.7 times the free-nucleon spin g factor. The g factor of the $g_{7/2}$ proton is thus $\sim$0.84 in the two shell-model calculations and 0.677 in the QRPA, mainly due to the difference in the δg_l values. Once these differences are considered, the QRPA can be brought into agreement with the shell model. In contrast, the Monte Carlo shell model (MCSM) [4] used the same $M1$ operator as the QRPA, so the difference in predicted g factors for these two models implies a difference between the wave functions, which requires further investigation, particularly as the MCSM calculation is two standard deviations below the measured g factor.

The g factors of the longer-lived 4_1^+ and 6_1^+ states in ^{134}Te have been measured previously [19,20]. To the extent that these states can be associated with pure $\pi(g_{7/2})^2$ configurations, their g factors should be the same as those of the 2_1^+ state. Simple rules then also govern the $E2$ transitions connecting these states.

Additional shell-model calculations, using OXBASH [21], were therefore performed to enable comparisons of $E2$ transition rates along with g factors in ^{134}Te. The interactions and model space were those of Brown *et al.* [3], but the empirical $M1$ operator of Jakob *et al.* [1] was used. $E2$ transition rates were evaluated using an effective proton charge of $e_p = 1.5e$. Calculations were performed for the full model space, which included all orbits in the major shell ($g_{7/2}$, $d_{5/2}$, $s_{1/2}$, $h_{11/2}$, $d_{3/2}$), and also for the simplified case wherein the two protons were restricted to the $g_{7/2}$ orbit.

The calculation in the restricted basis serves two purposes. First, by comparison with the calculations in the full valence space, the $\pi(g_{7/2})^2$ model gives a reference to measure the importance of configuration mixing in the valence space. Second, it also provides a benchmark for the particle-vibration model calculations to be discussed below, which aim to test the impact of ^{132}Sn core vibrations on the low-excitation structure of ^{134}Te. Both the large-basis shell model and the particle-vibration model collapse to the $\pi(g_{7/2})^2$ model in their limiting cases. It therefore provides a common link between these two models, which taken together allow an assessment of the quality of ^{132}Sn as an inert double-magic core.

The results of the calculations are presented in Fig. 5. The shell model accurately predicts the experimental g factors and points to rather pure $\pi(g_{7/2})^2$ configurations for the 2_1^+, 4_1^+, and 6_1^+ states in ^{134}Te. However, this conclusion is challenged by the $B(E2)$ data, where the shell model is in excellent agreement with experiment for the $6_1^+ \rightarrow 4_1^+$ and $4_1^+ \rightarrow 2_1^+$ transitions, but the theory falls short by $\sim$30% for the $2_1^+ \rightarrow 0_1^+$ transition.

Adjusting the proton effective charge cannot account for this added collectivity in the 2_1^+ state without spoiling the agreement for the decays of the 4_1^+ and 6_1^+ states. In the following discussion we therefore consider the effect of core excitations on the $E2$ transitions and g factors.

The first excited state of ^{132}Sn at 4.041 MeV is a 2^+ state, with an $E2$ transition strength to the ground state of 7(3) W.u. [22,23]. The effect of this core excitation on the valence nucleons was evaluated by performing particle-vibration model calculations in which two $g_{7/2}$ protons were coupled to a 2^+ core vibration using the formalism of Heyde and Brussaard [24]. The excitation energy and $E2$ transition strength of the 2_1^+ state in ^{132}Sn set the parameters of the core vibration. Nucleon-nucleon interactions were described by a surface-δ interaction. The strength of the coupling between valence nucleons and the core vibration was set to $\xi = 1.5$, a value applicable for nuclei with $A \sim 140$ [24]. The $E2$ transitions were evaluated using $e_p = 1.3e$, a value somewhat smaller than that needed in the absence of core excitations, as expected. No attempt was made to further tune the parameters. In the limit of no coupling between the valence nucleons and the core, the particle-vibration wave functions become identical to the restricted shell model with the two protons confined to $\pi g_{7/2}$.

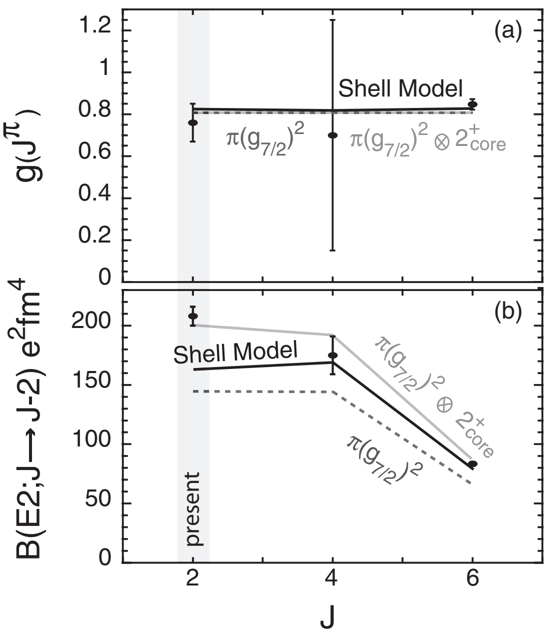

FIG. 5. Electromagnetic properties of the 2_1^+, 4_1^+, and 6_1^+ states in ^{134}Te: (a) g factors and (b) $B(E2; J \rightarrow J-2)$. The dark solid line shows the shell-model calculation in the full valence space, including all proton orbits in the major shell between $Z = 50$ and $Z = 82$. The dashed line is the shell model with the two protons restricted to the $\pi g_{7/2}$ orbit. The gray line is a particle-vibration model calculation in which two protons in $\pi g_{7/2}$ are coupled to the 2_1^+ excitation of ^{132}Sn.

Results of the particle-vibration calculations are shown in Fig. 5. The g factors are affected very little by the core vibration, but the $E2$ transition strengths are increased significantly, especially for the $2_1^+ \rightarrow 0_1^+$ transition. Coupling between the core vibration and the valence nucleons accounts for the shortfall in the shell-model calculation for the $2_1^+ \rightarrow 0_1^+$ transition. We therefore have clear evidence that the single-particle orbits outside ^{132}Sn are affected by vibrations of the core. Nevertheless, the influence on the wave functions of the states in ^{134}Te, and hence the g factors, is small. The 2_1^+ state remains $\sim$95% $\pi(g_{7/2})^2$, while the 4_1^+ and 6_1^+ states are $\sim$98% $\pi(g_{7/2})^2$.

To sum up, we have measured the g factor of the 2_1^+ state in the $N = 82$ nucleus ^{134}Te simultaneously with a precise measurement of $B(E2; 0_1^+ \rightarrow 2_1^+)$. Differences in theoretical predictions for $g(2_1^+)$ arise because the g factor is sensitive to both the wave function and the $M1$ operator. When an appropriate $M1$ operator is used, the electromagnetic properties of the low-excitation states of ^{134}Te are generally well described by the shell model, even in the approximation that the two protons are restricted to the $g_{7/2}$ orbit. However, there is evidence of additional quadrupole collectivity in the 2_1^+ state that can be attributed to coupling between the two valence protons and excitations of the ^{132}Sn core. The present work demonstrates the power of combined $B(E2)$ and RIV g-factor measurements on radioactive beams.

The authors thank the HRIBF operations staff for developing and providing the stable and radioactive beams used in this study, and J. P. Greene (Argonne National Laboratory) for making the carbon target. This research was sponsored by the Office of Nuclear Physics, U.S. Department of Energy, by the Australian Research Council under Grant No. DP0773273, by CONACyT (Mexico) Grant No. CB103366, and by the National Science Foundation. This work was also supported in part by the U.S. DOE under Contracts No. DE-AC05-76OR00033 (UNIRIB), No. DE-FG02-96ER40963 (UTK), and No. DE-FG52-08NA28552 (Rutgers).

[1] G. Jakob, N. Benczer-Koller, G. Kumbartzki, J. Holden, T. J. Mertzimekis, K.-H. Speidel, R. Ernst, A. E. Stuchbery, A. Pakou, P. Maier-Komor, A. Macchiavelli, M. McMahan, L. Phair, and I. Y . Lee, Phys. Rev. C **65**, 024316 (2002).

[2] J. Terasaki, J. Engel, W. Nazarewicz, and M. Stoitsov, Phys. Rev. C **66**, 054313 (2002).

[3] B. A. Brown, N. J. Stone, J. R. Stone, I. S. Towner, and M. Hjorth-Jensen, Phys. Rev. C **71**, 044317 (2005).

[4] N. Shimizu, T. Otsuka, T. Mizusaki, and M. Honma, Phys. Rev. C **70**, 054313 (2004).

[5] N. J. Stone, A. E. Stuchbery, M. Danchev, J. Pavan, C. L. Timlin, C. Baktash, C. Barton, J. Beene, N. Benczer-Koller, C. R. Bingham, J. Dupak, A. Galindo-Uribarri, C. J. Gross, G. Kumbartzki, D. C. Radford, J. R. Stone, and N. V. Zamfir, Phys. Rev. Lett. **94**, 192501 (2005).

[6] J. M. Allmond, D. C. Radford, C. Baktash, J. C. Batchelder, A. Galindo-Uribarri, C. J. Gross, P. A. Hausladen, K. Lagergren, Y. Larochelle, E. Padilla-Rodal, and C.-H. Yu, Phys. Rev. C **84**, 061303(R) (2011).

[7] J. M. Allmond, A. E. Stuchbery, D. C. Radford, A. Galindo-Uribarri, N. J. Stone, C. Baktash, J. C. Batchelder, C. R. Bingham, M. Danchev, C. J. Gross, P. A. Hausladen, K. Lagergren, Y. Larochelle, E. Padilla-Rodal, and C.-H. Yu, Phys. Rev. C **87**, 054325 (2013).

[8] G. J. Kumbartzki, N. Benczer-Koller, D. A. Torres, B. Manning, P. D. O'Malley, Y. Y. Sharon, L. Zamick, C. J. Gross, D. C. Radford, S. Q. J. Robinson, J. M. Allmond, A. E. Stuchbery, K.-H. Speidel, N. J. Stone, and C. R. Bingham, Phys. Rev. C **86**, 034319 (2012).

[9] D. C. Radford, C. Baktash, J. R. Beene, B. Fuentes, A. Galindo-Uribarri, C. J. Gross, P. A. Hausladen, T. A. Lewis, P. E. Mueller, E. Padilla, D. Shapira, D. W. Stracener, C.-H. Yu, C. J. Barton, M. A. Caprio, L. Coraggio, A. Covello, A. Gargano, D. J. Hartley, and N. V. Zamfir, Phys. Rev. Lett. **88**, 222501 (2002).

[10] C. J. Barton, M. A. Caprio, D. Shapira, N. V. Zamfir, D. S. Brenner, R. L. Gill, T. A. Lewis, J. R. Cooper, R. F. Casten, C. W. Beausang, R. Krücken, and J. R. Novak, Phys. Lett. B **551**, 269 (2003).

[11] A. Galindo-Uribarri, AIP Conf. Proc. **1271**, 180 (2010); www.phy.ornl.gov/hribf/research/equipment/hyball.

[12] C. J. Gross, T. N Ginter, D. Shapira, W. T. Milner, J. W. McConnell, A. N. James, J. W. Johnson, J. Mas, P. F. Mantica, R. L. Auble, J. J. Das, J. L. Blankenship, J. H. Hamilton, R. L. Robinson, Y. A. Akovali, C. Baktash, J. C. Batchelder, C. R. Bingham, M. J. Brinkman, H. K. Carter, R. A. Cunningham, T. Davinson, J. D. Fox, A. Galindo-Uribarri, R. Grzywacz, J. F. Liang, B. D. MacDonald, J. MacKenzie, S. D. Paul, A. Piechaczek, D. C. Radford, A. V. Ramayya, W. Reviol, D. Rudolph, K. Rykaczewski, K. S. Toth, W. Weintraub, C. Williams, P. J. Woods, C.-H. Yu, and E. F. Zganjar, Nucl. Instrum. Methods Phys. Res. Sect. A **450**, 12 (2000).

[13] A. E. Stuchbery, Nucl. Phys. **A723**, 69 (2003).

[14] S. Raman, C. W. Nestor, Jr., and P. Tikkanen, At. Data Nucl. Data Tables **78**, 1 (2001).

[15] M. Danchev, G. Rainovski, N. Pietralla, A. Gargano, A. Covello, C. Baktash, J. R. Beene, C. R. Bingham, A. Galindo-Uribarri, K. A. Gladnishki, C. J. Gross, V. Yu. Ponomarev, D. C. Radford, L. L. Riedinger, M. Scheck, A. E. Stuchbery, J. Wambach, C.-H. Yu, and N. V. Zamfir, Phys. Rev. C **84**, 061306(R) (2011).

[16] A. E. Stuchbery and N. J. Stone, Phys. Rev. C **76**, 034307 (2007).

[17] A. E. Stuchbery, A. Nakamura, A. N. Wilson, P. M. Davidson, H. Watanabe, and A. I. Levon, Phys. Rev. C **76**, 034306 (2007).

[18] N. J. Stone, At. Data Nucl. Data Tables **90**, 75 (2005).

[19] C. Goodin, N. J. Stone, A. V. Ramayya, A. V. Daniel, J. R. Stone, J. H. Hamilton, K. Li, J. K. Hwang, Y. X. Luo, J. O. Rasmussen, A. Gargano, A. Covello, and G. M. Ter-Akopian, Phys. Rev. C **78**, 044331 (2008).

[20] A. Wolf and E. Cheifetz, Phys. Rev. Lett. **36**, 1072 (1976).

[21] B. A. Brown, A. Etchegoyen, N. S. Godwin, W. D. M. Rae, W. A. Richter, W. E. Ormand, E. K. Warburton, J. S. Winfield, L. Zhao, and C. H. Zimmerman, *Oxbash for Windows PC*, Michigan State University Report no. MSU-NSCL 1289 (2004).

[22] J. R. Beene, R. L. Varner, C. Baktash, A. Galindo-Uribarri, C. J. Gross, J. Gomez del Campo, M. L. Halbert, P. A. Hausladen, Y. Larochelle, J. F. Liang, J. Mas, P. E. Mueller, E. Padilla-Rodal, D. C. Radford, D. Shapira, D. W. Stracener, J.-P. Urrego-Blanco, and C.-H. Yu, Nucl. Phys. A **746**, 471 (2004).

[23] D. C. Radford, C. Baktash, J. R. Beene, B. Fuentes, A. Galindo-Uribarri, J. Gomez del Campo, C. J. Gross, M. L. Halbert, Y. Larochelle, T. A. Lewis, J. F. Liang, J. Mas, P. E. Mueller, E. Padilla, D. Shapira, D. W. Stracener, R. L. Varner, C.-H. Yu, C. J. Barton, M. A. Caprio, D. J. Hartley, and N. V. Zamfir, Nucl. Phys. A **746**, 83 (2004).

[24] K. Heyde and P. J. Brussaard, Nucl. Phys. A **104**, 81 (1967).